Acta Materialia 131 (2017) 48–56

Contents lists available at ScienceDirect

Acta Materialia

journal homepage: www.elsevier.com/locate/actamat

Full length article

# Role of twin and anti-phase defects in MnAl permanent magnets☆

Simon Bance [a, *], Florian Bittner [b], Thomas G. Woodcock [b], Ludwig Schultz [b], Thomas Schrefl [c]

[a] Seagate Technology, 1 Disc Drive, Springtown, Derry, BT48 0BF Northern Ireland, UK
[b] IFW Dresden, Institute for Metallic Materials, Helmholtzstraße 20, 01069 Dresden, Germany
[c] Center for Integrated Sensor Systems, Danube University Krems, Viktor Kaplan Str. 2E, 2700 Wiener Neustadt, Austria

ARTICLE INFO

*Article history:*
Received 13 February 2017
Received in revised form
30 March 2017
Accepted 2 April 2017
Available online 5 April 2017

*2010 MSC:*
82D40

*Keywords:*
Permanent magnets
Twin defects
Anti-phase boundaries

ABSTRACT

We quantify and explain the effects of both anti-phase boundaries and twin defects in as-transformed τ-MnAl by carrying out micromagnetic simulations based closely on the results of microstructural characterization. We demonstrate that magnetic domain walls nucleate readily at anti-phase boundaries and are strongly pinned by them, due to anti-ferromagnetic coupling. Likewise, twin boundaries reduce the external field required to nucleate domain walls and provide strong pinning potentials, with the pinning strength dependent on the twinning angle. The relative strengths of the known twin defect types are quantified based on the anisotropy angles across their boundaries. Samples that have undergone heat treatment are imaged using electron back-scatter diffraction. The precise crystallographic orientation is mapped spatially and converted into a number of realistic finite element models, which are used to compute the effects of large concentrations of twin domains in a realistic morphology. This is shown to have a negative effect on the remanence coercivity and squareness. The maximum energy product $(BH)_{max}$ is therefore significantly lower than the theoretical limit of the material and much lower than MnAl permanent magnets that have been further processed to remove twin defects. The knowledge gained in this study will allow the optimization of processing routes in order to develop permanent magnets with enhanced magnetic properties.



## 1. Introduction

In the recent search for new rare-earth-free hard magnetic phases MnAl has gained particular attention due to the low cost and high abundance of the raw materials required [1,2]. While not able to compete with the incredible performance of sintered Nd-Fe-B permanent magnets, which can have high maximum energy products above $(BH)_{max} = 400$ kJ/m$^3$ (50 MGOe), MnAl, which has an estimated upper limit of $(BH)_{max} \approx 100$ kJ/m$^3$, could form the basis of a low cost class of general purpose permanent magnets with good machineability, to compete with polymer bonded Nd-Fe-B or ferrites [3,4].

A plot of approximate $(BH)_{max}$ versus raw material price in $/kg for various permanent magnet products is given in Fig. 1.[1] Typical $(BH)_{max}$ values and information on composition are collected from the existing literature and from manufacturer data, depending on availability [5–10]. It should be noted that although Sm-based magnets turn out to be quite competitive as mid-performing permanent magnets, the critical supply status of Sm (as with all rare earths) means that the price is likely to increase.

The proposed MnAl magnets consist of grains of the $L1_0$-structured τ phase, which is characterized by the presence of crystalline defects such as twins [11–13], of which there are three different types [14] and anti-phase boundaries (APBs) [15,16]. The microstructure is highly sensitive to the metallurgical state of the material. APBs are observed after the phase formation but are absent in hot deformed magnets [12] and the population of 2 of the 3 different twin-like defects is remarkably reduced in the hot

☆ A significant amount of this work was performed while at; Department of Technology, St Pölten University of Applied Sciences, St Pölten, Austria.

* Corresponding author.
*E-mail address:* simon.bance@seagate.com (S. Bance).

[1] Prices are estimated from the volume-fraction-adjusted market prices of the pure constituent materials alone (without considering any other manufacturing costs) except for the ferrites $BaFe_{12}O_{19}$ and $SrFe_{12}O_{19}$ where the current market prices for the required amount of precursors, $BaCO_3$ and $SrCO_3$ are used.

http://dx.doi.org/10.1016/j.actamat.2017.04.004
1359-6454/

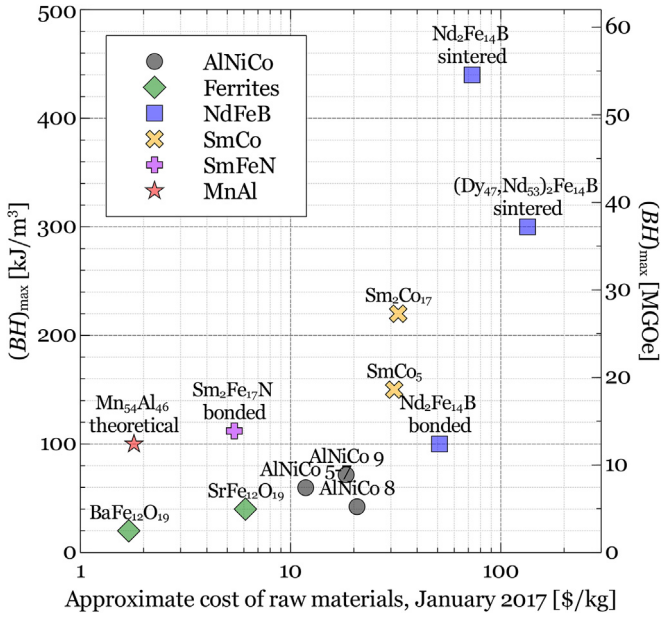


**Fig. 1.** Room temperature $(BH)_{max}$ as a function of approximate raw material costs for the theoretical MnAl permanent magnet and experimental values for a selection of common commercial permanent magnets. The raw material costs are a good indication of the relative cost of the manufactured magnets.

deformed state [14].

In the initial material, after the formation of the τ phase the coercivity is comparably low, which has been attributed to the presence of APBs [17]. APBs may be responsible for easy nucleation of domain walls but also act as domain wall (DW) pinning potentials, due to a local reduction of the domain wall energy across an APB [16]. APBs are created by a shear of the lattice of 1/2 [101] and this leads to a shorter atomic spacing between Mn atoms at the boundary, which may give rise to anti-ferromagnetic (AFM) coupling. This divides the crystal into two anti-parallel ferromagnetic regions.

Furthermore the impact of the complicated twinned structure on the magnetic properties may act as pinning centers for domain walls [11,18]. The orientation of the easy axis changes when crossing the twin boundary and the misorientation angle depends on the type of twin boundary. The strength of pinning interaction of the 3 different types of twins with magnetic domain walls may therefore be different and until now have not been determined. Knowledge of this is a vital step in the development of rare-earth free MnAl magnets.

The aim of the current work is to understand and quantify the interaction of APBs and twins with domain walls in as-transformed τ-MnAl by carrying out micromagnetic simulations based closely on the results of microstructural characterization. The knowledge gained in this study will allow the optimization of processing routes in order to develop permanent magnets with enhanced magnetic properties.

## 2. Experimental work

A binary Mn-Al alloy with the nominal composition $Mn_{54}$ $Al_{46}$ (at.%) was prepared by arc melting 99.99% pure Mn and Al under Ar atmosphere. The composition of the ingot was checked using chemical analysis and it was found that the difference between nominal and actual composition was below 1 at.%.

As the cast material consists of a mixture of τ and equilibrium $\gamma_2$ phases, a homogenization heat treatment at 1100 °C for 5 days followed by quenching was carried out. For this, the as-cast material was encapsulated in a glass tube which was evacuated to $10^{-4}$ mbar and then filled with 150 mbar of pure Ar.

After homogenization, the microstructure of the material was investigated using a Gemini Leo 1530 Scanning Electron Microscope (SEM) and is shown in Fig. 2 (a) in backscattered electron contrast. The microstructure consists of irregularly shaped grains and many planar interfaces, as was observed for C-doped MnAl elsewhere [14]. It should be noted that no indication of the occurrence of phases other than τ was found using microscopy or with X-ray diffraction measurements.

Electron backscatter diffraction (EBSD) was used to determine the local crystallographic orientation at individual points on the sample. A regular grid of measurement points with a spacing of 500 nm was chosen in the analysis region, yielding in total 40,000 data points. The resulting map of easy axis orientation is shown in Fig. 2b, represented by the angle from the out-of-plane axis. From the EBSD data, the interface distribution was calculated from the misorientation of neighboring data points. It was found that the so-called “true” twins have an angle of misorientation between the magnetically easy, crystallographic c-axis on either side of the twin boundary equal to θ = 75.6° [14]. The spatial distribution of true twin and other grain boundaries is visualized in Fig. 2c. Approximately 36% of the total interface length is represented by true twins.

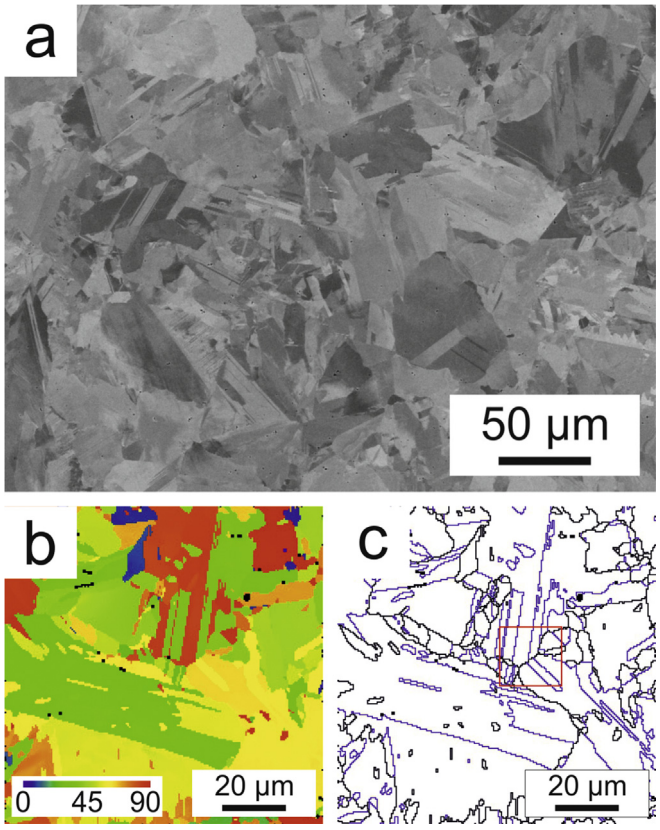


**Fig. 2.** Microstructure of $Mn_{54}$ $Al_{46}$ after homogenization at 1100 °C for 5 days and subsequent quenching into water: (a) Backscattered electron image, (b) EBSD map showing the orientation of the c-axis of τ with respect to the out of plane direction, (c) EBSD grain boundary map showing true twin (blue) with misorientation of the c-axis of θ = 75.6° and other grain boundaries (black) (The red rectangle shows the region which was used for simulation). (For interpretation of the references to colour in this figure legend, the reader is referred to the web version of this article.)